

Research on Terahertz Detector Based on Graphene Nanoribbon and Micron Ribbon

Shengmei He^{1,2}, Shuming Yang^{1,2,#}, Ze Zhang^{1,2}, Peirui Ji^{1,2} and Wei Chengyi^{1,2}

¹ State Key Laboratory for Manufacturing Systems Engineering, International Joint Laboratory for Micro/Nano Manufacturing and Measurement Technologies, Xi'an Jiaotong University, Xi'an 710049, China.

² School of Mechanical Engineering, Xi'an Jiaotong University, Xi'an 710049, China.

Corresponding Author / Email: shuming.yang@mail.xjtu.edu.cn, TEL: +86-139-9137-4172

KEYWORDS: Terahertz detection, Terahertz plasmon, FDTD, Graphene nanoribbon, Graphene micron ribbon

Terahertz detection technology has great significance in security detection, radar detection, data communication, biomedicine and astronomical observation. With the rapid development of technology in various fields, higher requirements are put forward for terahertz detectors. In order to solve the problems of low temperature, low sensitivity and complex structure of terahertz direct detectors, the research of terahertz direct detectors based on graphene nanoribbons and micro ribbons is carried out in this paper. Graphene is prepared into a strip array structure and the energy gap is adjusted to excite the SPPs of graphene for terahertz direct detection. Firstly, the excitation and regulation of terahertz plasmons are studied. Secondly, the terahertz detector device model based on graphene strip array is designed, and the influence of various structural parameters of the device on the resonant frequency of the device is simulated and analyzed using the FDTD, which provides effective structural parameters for the device preparation. The simulation results show that graphene ribbons can effectively improve the absorption of terahertz wave, and the optical response to different frequency points can be achieved by designing the width and period of graphene ribbons and Fermi energy levels. Finally, the fabrication process of terahertz detector based on graphene nanoribbon and micron ribbon is designed, and the structure models of the detector is completed. The electrical characteristics of the device are tested, and the regulation effect of gate voltage on device response is verified, which provides a basis for further research on THz detector.

NOMENCLATURE

W = the width of graphene microbands and nanoribbons

T = Periods of graphene microbands and nanoribbons

H = The dielectric layer thickness of the detector

1. Introduction

Terahertz refers to the electromagnetic wave with a frequency in the range of 0.1-10 terahertz, and its frequency range is between microwave and infrared¹. Terahertz wave has unique transient coherence, broadband and other excellent characteristics, making it widely used in military^{2,3}, aviation⁴, communications^{5,6}, medical^{7,8} and environmental⁹ fields. However, due to the special position of terahertz band in the spectrum, there are some obstacles in the research of terahertz devices. Moreover, the energy of atmospheric background thermal noise is similar to that of terahertz photons,

which is easy to cause interference. The existing terahertz detectors have problems such as slow response speed, complex structure, large volume, low temperature operation and poor adjustability. It is of great academic significance and practical value to study new high-performance terahertz detection technology^{10,11}.

In this paper, graphene strip array is designed to excite SPPs, and field effect tube structure is used to detect terahertz band. FDTD is used to simulate the influence of the device structure on the detector performance, and the device is designed and fabricated. Finally, the electrical characteristics are tested to prove the tuning effect of the gate voltage on the device.

2. Device modeling and simulation analysis

2.1 Excitation and regulation of graphene plasmons

Because graphene is almost transparent, the interaction between matter and light is very weak. SPPs have a strong local field enhancement effect, so they can be used to enhance the interaction

between light and graphene, and effectively confine the electromagnetic field energy to the range less than the wavelength near the interface. The graphene plasmon has the advantages of low loss and can change the Fermi level by doping or changing the gate voltage to regulate the graphene plasmon. Since the wave vector of graphene plasmon is much larger than the light wave vector at the same frequency, in order to be able to excite the surface plasmon, the graphene thin film is cut into a strip array structure. This method can increase the wave vector of graphene plasmon to achieve momentum matching¹. From the dispersion relationship of plasmons on the surface of graphene, it can be known that SPPs are related to the dielectric constant of the surrounding medium of the environment where graphene is located, the material characteristics of graphene, and the Fermi level of graphene. The resonance frequency can be adjusted by changing the gate voltage or doping graphene. For the graphene strip array, when light is incident on the graphene strip, surface plasmons will be excited on both sides of the strip, and interference will be formed through the reflection of the boundary. And the resonance frequency is related to the graphene band width and Fermi level¹². Based on the plasmon effect of graphene, the graphene nanoband and micro band field effect tube detector models are constructed. Graphene strip is a channel material. When free space light is incident, the two-dimensional electron gas in the channel generates plasmons under terahertz wave radiation. The nonlinear plasma propagates in the channel, causing a voltage difference between the source and drain. The optical signal is converted into an electrical signal to realize photoelectric detection.

2.2 Detector simulation analysis

The finite difference time domain method is used to simulate and analyze the device, and the simulation model of graphene terahertz photodetector is constructed as shown in Figure 1. The bottom layer is a S_1 substrate and a S_1O_2 dielectric layer. Above the dielectric layer is a single-layer graphene strip film. The graphene is set as 2D material. The X direction is a periodic boundary, the Y direction is a symmetric boundary condition, and the Z direction is a PML boundary. Set the light source as plane light, with vertical incidence and frequency of 0.1THz-1THz.

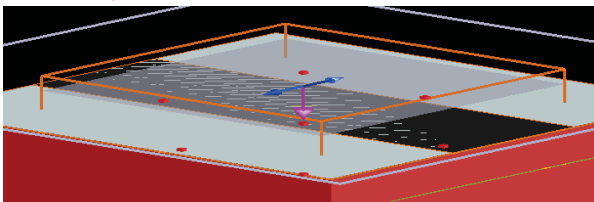


Fig. 1 Simulation model diagram

Set $W = 100\mu m$, $E_F = 0.64eV$, and Fig. 2 is the simulation results. It can be seen from the transmission spectrum figure 2(a) that the transmission valley appears at about 0.42 THz, which indicates that when the light is incident at about 0.42 THz, the incident light is strongly coupled with the free electrons on the graphene surface, and the incident light energy is converted into SPPs, so the transmittance is the lowest. When deviating from the resonance frequency, i.e., detuning, the transmittance increases, i.e., the SPPs intensity

decreases. It can be seen from the cross-sectional electric field distribution figure 2(b) that the device has an obvious field strength enhancement effect in the graphene strip layer. Fig. 2(c) shows the surface field intensity distribution of graphene when the terahertz wave with the incident light frequency of 0.1, 0.4 and 1 THz is vertically incident. It can be seen from the figure that SPPs are mainly concentrated at the edges of graphene. When SPPs propagate back and forth between the boundaries of graphene, they will interfere with each other. The intensity of SPPs is 2-3 times that of the middle part of graphene micro ribbon. With the increase of detuning degree, the field intensity distribution gradually weakens¹³.

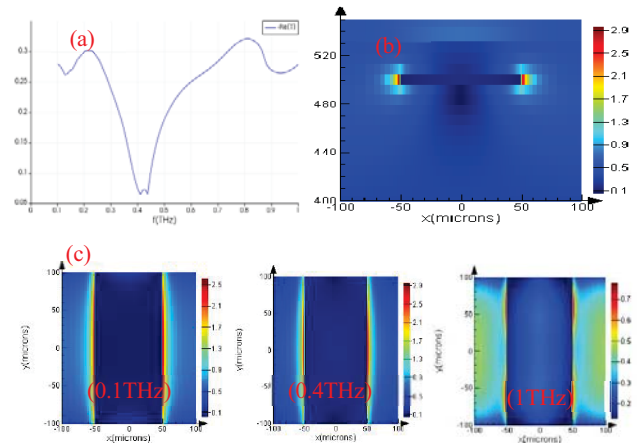


Fig. 2 $W=100\mu m$, $E_F=0.64eV$ simulation results. (a) Transmission spectrogram. (b) Cross-section electric field distribution diagram. (c) Surface electric field distribution map.

The effects of graphene band width, band period, dielectric layer thickness and graphene Fermi level on the resonant frequency of the device are simulated and analyzed. The results are shown in Fig. 3. It can be seen from Fig. 3(a) that the device has obvious transmission Valley at about 0.13 THz and 0.4 THz. With the increase of the micron band width, the resonance frequency of the device has a blue shift phenomenon. Similarly, it can be seen from Fig. 3(b) that as the band period increases from 150um to 250um, the transmission valley of the device appears blue shift. It can be seen from Fig. 3(c) that the thickness of the dielectric layer has little influence on the resonance frequency of the device. Fig. 3(d) shows that the resonance frequency of the plasmon on the graphene surface is related to the Fermi level. Since the Fermi level of graphene is directly proportional to the arithmetic square root of the graphene carrier concentration, the Fermi level of graphene can be changed by adjusting the graphene carrier concentration to achieve the effect of adjusting the resonance frequency. It can be seen from the Fig. 3(d) that the graphene Fermi level has a great influence on the resonance frequency. As the graphene Fermi level increases from 0.3eV to 0.7eV, the absorption peak of the device gradually shifts red. This is because the Fermi level of graphene changes, the carrier concentration in graphene will change with it, and the resonance frequency of its carriers will also change. It is proved that the resonance frequency of graphene can be adjusted by adjusting the Fermi level. The simulation shows that the graphene band width and Fermi level can effectively adjust the

resonant frequency of the detector. By changing the band size and Fermi level of graphene, the effective response to different frequency points can be achieved.

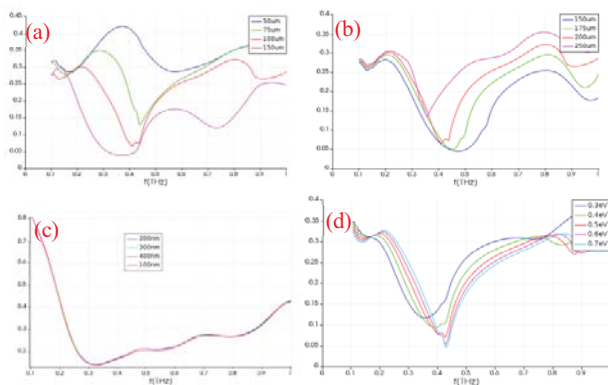


Fig. 3 The influence of different structural parameters on resonant frequency. (a) Transmission spectra for different W. (b) Transmission spectra for different T (c) Transmission spectra for different H. (d) Transmission spectra for different E_F .

3. Preparation of detectors and electrical tests

3.1 Key process steps of device preparation

The detector is based on p-type doped silicon with a thickness of 500 μm . The dielectric layer is SiO_2 with a thickness of 300 nm. The channel layer of the FET is graphene nanoribbons and graphene micro ribbons with different sizes. The main preparation process steps are as follows. Fig. 4 is a physical structure of the device.

(1) Preparation of back electrode. The back electrode was evaporated on the back of the p-type doped silicon wafer using an electron beam evaporation table, and the electrode were 20nm Gr and 80nm Au. The role of Cr is to enhance the adhesion between Au and Si substrate.

(2) Preparation of source drain electrode. Using an ultraviolet lithography machine and a prepared chromium plating mask, the source drain electrode pattern is transferred to the surface of the sample, and the source drain electrode is evaporated using an electron beam evaporation stage after development.

(3) Cutting sample into single device by laser

(4) Transfer of graphene. Cut PMMA \ graphene to 0.5cm * 0.5cm small pieces ,put them into deionized water and transfer to the prepared sample pieces. After standing at room temperature for 30min, then werw placed on a hot plate at 70-100 $^{\circ}\text{C}$ for 30min to remove the water between graphene and the target substrate. Immerse the sample in three clean acetone solutions for 20min, 20min and 30min in order to remove the PMMA on the graphene surface to the maximum extent.

(5) Preparation of graphene ribbons. Nanoribbons are etched by electron beam and PMMA electron beam photoresist is used. Compared with other positive adhesives, PMMA has less damage to graphene. Draw the required nanoribbon pattern on the electron beam lithography machine, and then transfer it to the sample. The micron ribbon is etched with an ultraviolet lithography machine, and the graphene micro ribbon pattern on the mask is transferred to the

sample. After development, the relative position of the micro ribbon and the channel is observed with a light microscope to confirm that the graphene strip can be well located in the center of the channel.

(6) The graphene exposed after development was removed by oxygen plasma etching machine to form graphene micro ribbon and nanoribbon.

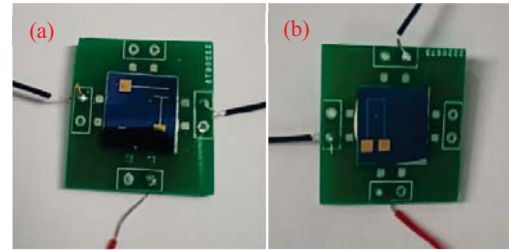


Fig. 4 Device physical structure diagram (a) Graphene micron Ribbon array detector (b) Graphene nanoribbon array detector

3.2 Measurement and analysis of electrical characteristics

The electrical characteristic test of graphene field effect tube photodetector mainly includes graphene transfer characteristic test and graphene output characteristic test. In this paper, the semiconductor device analyzer (B1500A) and triaxial probe table are used to test the transfer characteristics and output characteristics of the device. For the graphene transfer characteristic curve test, the fixed source drain voltage is 2V, and the gate voltage is scanned from 0V to 140V, as shown in Fig. 5(a). For the output characteristic curve test, fix a gate voltage, scan the source drain voltage from 0V to 2.5V, and obtain the curve of the current between the source and drain as a function of the source drain voltage, as shown in Fig. 5(b). The fixed gate voltages are 60V, 80V, 100V and 160V respectively. The electrical characteristics of the device are tested in the dark room of the semiconductor device analyzer, and the ambient temperature is 300K.

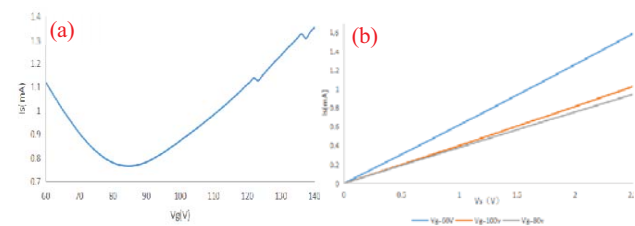


Fig. 5 Electrical characteristics test results (a) Transfer characteristic test results (b) Output characteristic test results

It can be seen from Fig. 5(a) that the prepared terahertz detector device has obvious gate voltage regulation characteristics. With the gradual increase of the gate voltage, the source drain current decreases first and then increases. The Dirac point voltage is about 83v, which indicates that the graphene is in the p-type doped state and heavily doped. The main reason is that the graphene will absorb water, nitrogen, oxygen and other impurities in the air during and after the transfer, and the graphene surface has been subjected to some process steps . These impurities will pollute the graphene and make the graphene appear as p-type doping. The transfer curve is asymmetric

with respect to the Dirac point, indicating that the mobility of holes and electrons in graphene are different, which is related to the molecular type of chemisorption on the surface of graphene. It can be seen from Fig. 5(b) that the source drain voltage and current show a perfect linear relationship, indicating that graphene and metal electrode have very good ohmic contact. In addition, it can be seen from the figure that when the gate voltage is 80V, the slope of the curve is the smallest, indicating that the graphene resistance is the largest, which corresponds to the graphene transfer characteristic curve. As a whole, the slope of I-V curve decreases first and then increases with the increase of gate voltage, that is, detector has the characteristics of gate voltage regulation.

3. Conclusions

In this paper, we use graphene strip array structure to excite graphene surface plasmons to detect terahertz waves. The effects of different device structures on the response frequency are analyzed theoretically and simulated. FDTD simulation results show that the graphene strip array layer on the device has an obvious field strength enhancement effect, and the band width, period and Fermi level of graphene strip array have a tuning effect on the terahertz wave response of the device, and the thickness of the dielectric layer has little effect. SPPs are mainly concentrated at the edge of graphene, and their intensity is 2-3 times that of the middle part of graphene micro belt. With the increase of detuning degree, the field intensity distribution gradually weakens. The detector models based on graphene micro ribbon and nanoribbon were designed and prepared. The graphene micro ribbon was prepared by ultraviolet lithography, and the graphene nanoribbon was prepared by EBL. Finally, the electrical characteristics of the detector are tested, and the test results show that the gate voltage has obvious regulation characteristics on the device.

ACKNOWLEDGEMENT

Thanks to the teachers and students of the research group for their help and guidance.

REFERENCES

1. Weiqing Yuan. "Research on Key Technologies of terahertz detector based on graphene nanogrid," D. Chongqing University, 2019
2. Guangkun Yang, Bin Yuan, Dongyan Xie, Xiaodan Shen. "Application of terahertz technology in military field," J. Laser and infrared, Vol. 41, No. 04, pp. 376-380, 2011.
3. Guozhong Zhao, Yanchun Shen, Ying Liu. "Application of terahertz technology in military and security fields," J. Journal of electronic measurement and instrumentation, Vol. 29, No. 08, pp. 1097-1101, 2015.
4. Bibo Min, Chang'e Zeng, Xin Yin, Junhai Ma. "Application of terahertz technology in military and aerospace fields," J. Journal of Terahertz Science and electronic information, Vol. 12 No. 03, pp. 351-354, 2014
5. Xin Zheng, Chao Liu. "Development of terahertz technology and its application in radar and communication systems," J. Journal of microwave, Vol. 27, No. 01, pp. 1-5, 2011.
6. KLEINE-OSTMANN T, NAGATSUMA T. "A review on terahertz communications research," J. Journal of Infrared, Millimeter, and Terahertz Waves, Vol. 32, No. 02, pp. 143-171, 2011.
7. SIEGEL P H. "Terahertz technology in biology and medicine," J. IEEE Transactions on Microwave Theory and Techniques, Vol. 52, No. 10, pp. 2438-2447, 2004
8. Jun Zou, Shenggang Liu. "Research progress of terahertz biomedical applications," J. Modern Applied Physics, Vol. 5, No. 2, pp. 85-97, 2014.
9. Yimin Lu, Jiachun Wang, Jiaming Shi, et al. "Application of terahertz technology in smoke and dust detection," J. Infrared and laser engineering, Vol. 39, No. 3, pp. 487-490, 2010.
10. Ferguson B., Zhang X. C. "Materials for terahertz science and technology," J. Physics. Vol. 1, No. 2, pp. 26-33, 2002.
11. Zhang X. C., Shkurinov A., Zhang Y. "Extreme terahertz science," J. Nature Photonics. Vol. 11, No. 1, pp. 16-18, 2017.
12. Yun Wang, Yi Lu, Haoyu Luo, Yan Ding. "Study on excitation and field distribution characteristics of graphene micro band and thzspps," J. Chinese Science: Physics and mechanics astronomy, Vol. 51, No. 3, pp. 83-89, 2021.
13. Du L, Tang D, Yuan X. "Edge-reflection phase directed plasmonic resonances on graphene nano-structures," Opt Express, Vol. 22, No. 19, pp. 22689-22698, 2014.